SEISMIC SIGNATURES OF FRACTURED RESERVOIRS: THEORY VERSUS NUMERICAL SIMULATIONS

1st Junxin Guo*
Curtin University
Perth, WA 6845
junxin.guo@postgrad.curtin.edu.au

2nd Stanislav Glubokovskikh
Curtin University
Perth, WA 6845
stanislav.glubokovskikh@curtin.edu.au

3rd Boris Gurevich
Curtin University &CSIRO
Perth, WA 684
B.Gurevich@curtin.edu.au

4th J. Germán Rubino
CONICET
San Carlos de Bariloche, Argentina
german.rubino@cab.cnea.gov.ar

SUMMARY

Seismic attenuation and dispersion usually occur in the fractured reservoirs. The wave-induced fluid flow (WIFF) is recognized as an important mechanism for these phenomena. In this work, we study the seismic attenuation and dispersion due to WIFF in saturated rocks containing two orthogonal sets of intersecting fractures. Based on the existing unified model for the WIFF, we proposed the theoretical model for three types of fractures: periodic planar fractures, randomly-spaced planar fractures, and penny-shaped cracks. The 2D synthetic rock sample with intersecting fractures is then studied by both numerical simulations and the proposed theoretical model. The numerical simulations are carried out using an upscaling method based on Biot's quasi-static equations of poroelasticity. We find a good agreement between the theoretical predictions and the numerical simulations. For the WIFF between fractures and the background, the seismic dispersion and attenuation predicted by the theoretical model for penny-shaped cracks are in best agreement with the numerical simulation results. On the other hand, for the WIFF between connected fractures, it turns out that the theoretical model for periodic planar fractures is best. The proposed theoretical approach can be applied to both 2D and 3D fracture systems, which can thus constitute a useful tool for the characterization of reservoirs with intersecting fractures.

Key words: Fracture intersection; Wave induced fluid flow; Seismic dispersion and attenuation

INTRODUCTION

Fractures are common features in the geological formations, which have great influence on both the hydraulic and mechanical properties of these formations. Hence, detection and characterization of the fractures are of great importance in many disciplines, such as oil/gas exploration and production, nuclear waste storage, among many others (e.g., Neuzil, 2013; Liu et al., 2017). To this end, the seismic method is often used due to its non-invasive feature and a relative large detection scale. As the resolution of the seismic data is usually not enough to image the fractures directly, the seismic attributes play an important role in the fracture detection and characterization. Especially, seismic dispersion and attenuation present special value for this purpose as the seismic wave usually experiences velocity dispersion and energy dissipation when propagating through the fractured formations. An important mechanism for such dispersion and attenuation is the wave-induced fluid flow (WIFF) between the fractures and the background medium (FB-WIFF) (e.g, Müller et al., 2010). Up until now, numerous models have been proposed to describe this mechanism (e.g., Chapman, 2003; Brajanovski et al., 2006; Galvin and Gurevich, 2006, 2007, and 2009; Guo, 2017a, 2017b).

Besides the FB-WIFF, in the recent studies of Rubino et al. (2013, 2014, and 2017), it is found that the WIFF also occurs within the connected fractures (FF-WIFF). It is shown that FF-WIFF can also result in significant seismic dispersion and attenuation. Hence, it is essential to study this mechanism in detail. However, to date, it is mainly studied through the numerical simulations and little theoretical analysis has been carried out. A recent work in this aspect was published by Guo et al. (2016), who quantified the elastic properties of saturated rocks containing two perpendicular sets of intersecting fractures theoretically in the low- and high- frequency limits as well as at the intermediate frequency range. The effects of FF-WIFF were taken into account in their work. In this paper, we extend their results to the full frequency range theoretically. To validate the applicability of the extension, the theoretical predictions are then compared with the corresponding numerical simulations.

METHOD

Here, we consider the saturated porous rocks with two perpendicular sets of intersecting fractures. Three types of fracture geometries are investigated: periodic planar fractures, randomly-spaced planar fractures, and penny-shaped cracks. When the seismic wave propagates through such rocks, it will induce the fluid pressure gradient not only between the fractures and the background medium, but also between the two perpendicular fracture sets (e.g., Rubino et al., 2013). Hence, both the FB-WIFF and FF-WIFF will occur, which will result in the seismic dispersion and attenuation. To describe the frequency-dependent stiffness coefficients caused by these two manifestations of WIFF, we can employ the unified model proposed by Gurevich et al. (2009) as follows:

$$\frac{1}{c^{sat}} = \frac{1}{C_1}\left[1+\left(\frac{C_1-C_0}{C_0}\right)/\left(1-\varsigma+\varsigma\sqrt{1-i\frac{\omega\tau}{\varsigma^2}}\right)\right], \tag{1}$$

where c^{sat} is the P-wave modulus in the direction perpendicular to the fracture plane; ω is the seismic wave angular frequency; ζ and τ are parameters that shape the P-wave dispersion and attenuation curves as functions of frequency; and C_0 and C_1 represent the values of the P-wave modulus in the low- and high- frequency limits of the FB-WIFF or FF-WIFF, respectively.

To calculate the values of ζ and τ, we first need to obtain the low- and high- frequency asymptotes of equation (1) as follows:

$$\frac{1}{c^{sat}} = \frac{1}{C_0}\left(1+i\omega T\right), \quad \omega\tau \ll \varsigma^2 \tag{2}$$

$$\frac{1}{c^{sat}} = \frac{1}{C_1}\left(1+\frac{G}{\sqrt{-i\omega}}\right). \quad \omega\tau \gg 1 \tag{3}$$

Once the values of T and G are known, ζ and τ can be computed as follows:

$$\tau = \left(\frac{C_1-C_0}{C_0 G}\right)^2, \tag{4}$$

$$\varsigma = \frac{\left(C_1-C_0\right)^3}{2C_1C_0^2TG^2}. \tag{5}$$

For the FB-WIFF, C_0 and C_1 can be calculated using the method described in Guo et al. (2016) and the expressions for T and G are as follows:

Periodic planar fractures:

$$T = \frac{1}{12}\frac{C_1-C_0}{C_1}\frac{\left(\frac{\phi_b}{\kappa_b}+\frac{\phi_c}{\kappa_c}\right)\eta H^2}{\frac{M_bL_b}{C_b\phi_b}+\frac{M_cL_c}{C_c\phi_c}}, \tag{6}$$

$$G = \frac{2S_1C_1\left(\frac{\alpha_bM_b}{C_b}-\frac{\alpha_cM_c}{C_c}\right)^2}{\sqrt{\frac{M_bL_b\eta}{C_b\kappa_b}}+\sqrt{\frac{M_cL_c\eta}{C_c\kappa_c}}}, \tag{7}$$

Penny-shaped cracks:

$$T = \frac{1}{5}\frac{C_1-C_0}{C_0}\frac{\left(2-4\alpha_bg_b+3\alpha_b^2g_b^2\right)a^2\eta}{g_b\left(1-g_b\right)L_b\kappa_b}, \tag{8}$$

$$G = \frac{2S_2C_1\left(\frac{\alpha_bM_b}{C_b}-\frac{\alpha_cM_c}{C_c}\right)^2}{\sqrt{\frac{M_bL_b\eta}{C_b\kappa_b}}+\sqrt{\frac{M_cL_c\eta}{C_c\kappa_c}}}, \tag{9}$$

where C_b and L_b are the P-wave modulus of the saturated and dry background, respectively; μ_b is the dry background shear modulus and g_b is the ratio of μ_b to L_b; κ_b is the permeability of the background; ϕ_b is the fraction of background with respect to the whole porous medium; α_b is the Biot's coefficient of the background; and M_b is the Biot's modulus of the background. The subscript c represents the corresponding values for the porous material infilling the fractures. For the penny-shaped cracks, a and ε are the crack radius and density, respectively. In addition, H represents the distance between consecutive planar fractures, and S_1 and S_2 are the specific fracture surface area per unit volume for planar fractures and penny-shaped cracks, respectively. Both the fractures and the background pores are saturated with the same fluid with viscosity η.

In the case of random distribution of the planar fractures, the value of T tends to infinity (ζ tends to zero), whereas G has the same expression as equation (7).

For the FF-WIFF, the values of C_0 and C_1 can also be obtained using the approach described in Guo et al. (2016). To calculate the values of the T and G, equations (6) – (9) can still be used. However, the properties of the background medium need to be replaced by those of an effective medium, which is composed of the fractures parallel to the wave propagation direction and the background

medium. The properties of the effective medium in the direction parallel to the wave propagation can then be substituted into equations (6) – (9) to obtain the values of T and G.

Hence, the P-wave modulus in the direction perpendicular to one of the fracture plane can be calculated in the full frequency range, considering the effects of both FB-WIFF and FF-WIFF. As this P-wave modulus is most influenced by the WIFF compared to the other stiffness coefficients, we only focus on this P-wave modulus in this paper. The values of the other stiffness coefficients can be calculated using the approach proposed by Galvin and Gurevich (2015), which will be studied in detail in the future.

RESULTS

To show the frequency-dependent P-wave modulus caused by the FB-WIFF and FF-WIFF, we consider a 2D synthetic sample with two sets of perpendicular intersecting fractures here, as shown in Figure 1. The sample has a dimension of 20 cm × 20 cm, which is saturated with water, with a bulk modulus of 2.25 GPa. The coordinate system is established, such that the x- and y- axis are perpendicular to the vertical and horizontal fractures, respectively. The length of the sample along z-axis is long enough to ensure that the plane strain condition is satisfied. Hence, the 3D problem can be reduced to the 2D problem. The two sets of fractures are oriented horizontally and vertically in the background medium, respectively. Both of them have 20 fractures. For the background medium, its properties are assumed as follows: porosity: 0.1, permeability: 10-4 mD, dry bulk modulus: 26 GPa, dry shear modulus: 31 GPa, grain bulk modulus: 37 GPa. For the fractures, they have a rectangular shape with a length of ~4 cm and a thickness of 0.06 cm. Inside the fractures, it is assumed that they are filled with a porous and compliant material with a dry bulk modulus of 0.04 GPa and a shear modulus of 0.02 GPa. The porosity and permeability of this material are 0.8 and 100 D, respectively. Furthermore, the grains composing the infill material is assumed to be same with those for the background medium.

Apart from the theoretical predictions of the P-wave modulus, we also carry out the numerical simulations for comparison and validation of the theoretical results. The numerical simulations employ an upscaling method based on the Biot quasi-static equations of poroelasticity, which was proposed by Rubino et al. (2016). Using the parameters presented above, both the theoretical predictions and the numerical simulations are then carried out and compared. It is important to mention here that, the effective elastic properties of the fracture infill material for the 2D sample need to be obtained during the theoretical predictions. The detail of this procedure can be found in Guo et al. (2017a, 2017b). In the following, we only show the results for C_{22} (in the direction along y-axis), as the behaviours of C_{11} and C_{22} with the frequencies are similar.

The dispersion and attenuation of C_{22} due to FB-WIFF are shown in Figures 2a and 2b, respectively. It can be found that the theoretical predictions by the model for the penny-shaped cracks agree with the results of the numerical simulations best. At low frequencies, the model for periodic planar fractures underestimates the attenuation, whereas that for the random case overestimates the attenuation. At high frequencies, the results by all the three models are similar to each other. This is due to the fact that, the energy primarily dissipates in the immediate vicinity of the fracture surface at high frequencies and hence the seismic dispersion and attenuation is controlled by the specific fracture surface area under this condition. As we use the specific fracture surface area of the real sample for all the three models, their results will then converge at high frequencies, which are in good agreement with the numerical simulations.

Figures 2c and 2d show the results for the dispersion and attenuation of C_{22} due to FF-WIFF. It can be found that FF-WIFF occurs at the frequency much higher than the FB-WIFF. This is due to the fact that the characteristic frequency for the FB-WIFF is controlled by the background medium permeability, whereas that for the FF-WIFF is determined by the permeability of the fracture infill material. Hence, the much higher permeability of the fracture infill material than the background medium results in the higher characteristic frequency for FF-WIFF. It is also interesting to find that instead of the penny-shaped model, the theoretical predictions by the model for the periodic planar fractures are in best agreement with the numerical simulations. This indicates that the fractures behaves in a way similar to that of the periodic planar fractures when the FF-WIFF occurs. Furthermore, it can be noted that the discrepancies between the theoretical predictions and the numerical simulations are larger than those for the FB-WIFF case. The possible reason is that equations (6) – (9) require that the background medium is isotropic, whereas the effective medium used for this case is anisotropic. We use the properties of the anisotropic effective medium in the wave propagation direction to replace the original isotropic background properties. This may result in the deviations of the theoretical predictions from the numerical simulations.

CONCLUSIONS

In this work, we propose a theoretical model to quantify the seismic attenuation and dispersion due to WIFF in saturated rocks containing two orthogonal sets of intersecting fractures. The approach is based on existing unified model for the WIFF. Three types of fracture geometries are considered: periodic planar fractures, randomly-spaced planar fractures, and penny-shaped cracks. Synthetic 2D rock sample with intersecting fractures is then studied by the proposed theoretical framework. To validate the theoretical prediction results, the numerical simulations are also carried out, which employs an upscaling method based on Biot's quasi-static equations of poroelasticity. Good agreement is found between the theoretical predictions and the numerical simulations. For the FB-WIFF, the seismic dispersion and attenuation predicted by the theoretical model for penny-shaped cracks agrees with the numerical simulation results best. However, for the FF-WIFF case, it turns out that the theoretical model for periodic planar fractures is best. The proposed theoretical approach can be applied to both 2D and 3D fracture systems, which can thus constitute a useful tool for the characterization of reservoirs with intersecting fractures.

ACKNOWLEDGMENTS

The authors are grateful to the sponsors of the Curtin Reservoir Geophysics Consortium (CRGC) for the financial support.

REFERENCES

Brajanovski, M., Gurevich, B., and Schoenberg, M., 2005, A model for P-wave attenuation and dispersion in a porous medium permeated by aligned fractures: Geophysical Journal International, 163, 372-384.

Chapman, M., 2003, Frequency dependent anisotropy due to mesoscale fractures in the presence of equant porosity: Geophysical Prospecting, 51, 369-379.

Galvin, R.J., and Gurevich, B., 2006, Interaction of an elastic wave with a circular crack in a fluid-saturated porous medium: Applied Physics Letter, 88, 061918.

Galvin, R.J., and Gurevich, B., 2007, Scattering of a longitudinal wave by a circular crack in a fluid-saturated porous medium: International Journal of Solids and Structures, 44, 7389-7398.

Galvin, R.J., and Gurevich, B., 2009, Effective properties of a poroelastic medium containing a distribution of aligned cracks: Journal of Geophysical Research: Solid Earth, 114, B07305.

Galvin, R.J., and Gurevich, B., 2015, Frequency-dependent anisotropy of porous rocks with aligned fractures: Geophysical Prospecting, 63, 141-150.

Guo, J., Rubino, J.G., Barbosa, N.D., Glubokovskikh, S., and Gurevich, B., 2017a, Seismic dispersion and attenuation in saturated porous rocks with aligned fractures of finite thickness: theory and numerical simulations – Part I: P-wave perpendicular to the fracture plane, Submitted to Geophysics.

Guo, J., Rubino, J.G., Barbosa, N.D., Glubokovskikh, S., and Gurevich, B., 2017b, Seismic dispersion and attenuation in saturated porous rocks with aligned fractures of finite thickness: theory and numerical simulations – Part II: Frequency-dependent anisotropy, Submitted to Geophysics.

Guo, J., Rubino, J.G., Glubokovskikh, S., and Gurevich, B., 2016, Effects of fracture intersections on seismic dispersion: theoretical predictions versus numerical simulations: Geophysical Prospecting, doi:10.1111/1365-2478.12474.

Gurevich, B., Brajanovski, M., Galvin, R.J., Müller, T.M., and Toms-Stewart, J., 2009, P-wave dispersion and attenuation in fractured and porous reservoirs - poroelasticity approach: Geophysical Prospecting, 57, 225-237.

Liu, C., Mehrabian, A., and Abousleiman, Y., 2017, Poroelastic dual-porosity/dual-permeability after-closure pressure-curves analysis in hydraulic fracturing: SPE J., 22, no.1, 198-218, doi: http://dx.doi.org/10.2118/181748-PA.

Müller, T.M., Gurevich, B., and Lebedev, M., 2010, Seismic wave attenuation and dispersion resulting from wave-induced flow in porous rocks – A review: Geophysics, 75, no.5, 75A147-75A164.

Neuzil, C.E., 2013, Can shale safely host U.S. nuclear waste?: EOS, Transactions, American Geophysical Union, 94, no. 30, 261-268.

Rubino, J.G., Caspari, E., Müller, T.M., and Holliger, K., 2017, Fracture connectivity can reduce the velocity anisotropy of seismic waves: Geophysical Journal International, 210, 223-227.

Rubino, J.G., Caspari, E., Müller, T.M., Milani, M., Barbosa, N.D., and Holliger, K., 2016, Numerical upscaling in 2D heterogeneous poroelastic rocks: Anisotropic attenuation and dispersion of seismic waves: Journal of Geophysical Research: Solid Earth, 121, 6698-6721, doi:10.1002/2016JB013165.

Rubino, J.G., Guarracino, L., Müller, T.M., and Holliger, K., 2013, Do seismic waves sense fracture connectivity?: Geophysical Research Letter, 40, 692-696.

Rubino, J.G., Müller, T.M., Guarracino, L., Milani, M., and Holliger, K., 2014, Seismoacoustic signatures of fractures connectivity: Journal of Geophysical Research: Solid Earth, 119, 2252-2271.

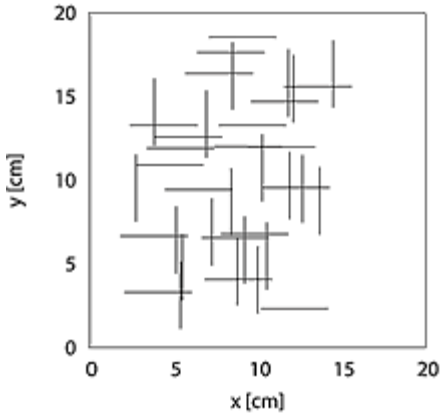

Figure 1: Geometry of the synthetic 2D sample with two sets of perpendicular intersecting fractures.

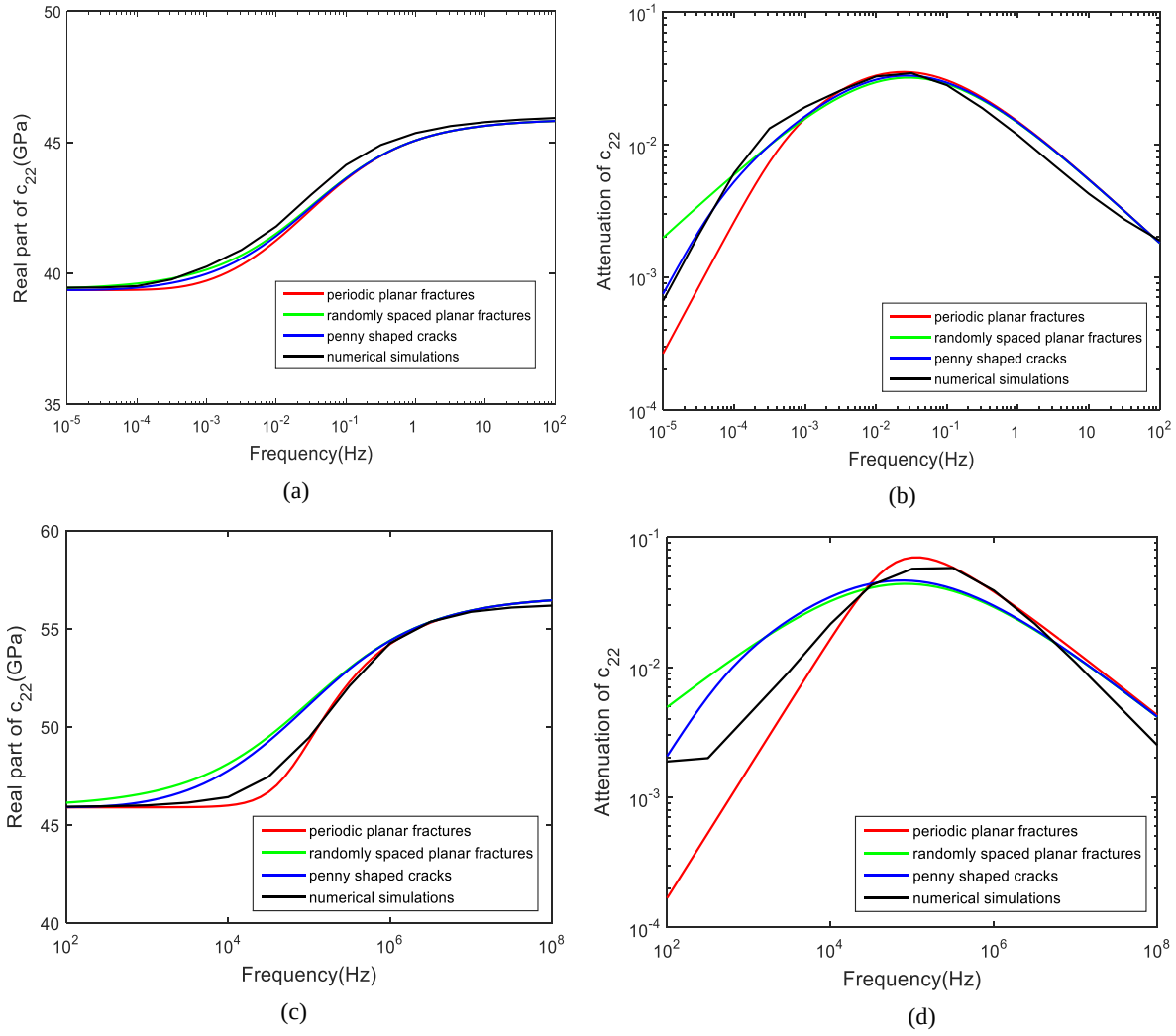

Figure 2: Dispersion and attenuation of C_{22}. (a) and (b) are the results caused by FB-WIFF, whereas (c) and (d) represent the results due to FF-WIFF.